

The geometry of sound rays in a wind

G. W. Gibbons¹ and C.M. Warnick^{1,2}

1. D.A.M.T.P., Cambridge, Wilberforce Road, Cambridge CB3 0WA, U.K.

2. Queens' College, Cambridge, CB3 9ET, U.K.

January 12, 2013

Abstract

We survey the close relationship between sound and light rays and geometry. In the case where the medium is at rest, the geometry is the classical geometry of Riemann. In the case where the medium is moving, the more general geometry known as Finsler geometry is needed. We develop these geometries ab initio, with examples, and in particular show how sound rays in a stratified atmosphere with a wind can be mapped to a problem of circles and straight lines.

1 Introduction: Propagation of Waves in Moving Media

Almost everyone must be familiar, by report at least, with optical mirages. In hot regions such as the desert, when the speed of light is greater at low altitudes than at higher altitudes, distant palm trees can appear inverted as if reflected off a cool pool of water in a nearby oasis, see Figure 1. It is less well known that in cold regions such as the arctic, where the opposite conditions prevail, distant ships can appear inverted in the sky, the light from them having been bent over an intervening iceberg, see Figure 2. More mundanely, motorway travellers on hot dry summer days often have the disconcerting impression that there are sheets of water lying on the road some distance ahead. The explanation of phenomena like this is easily understood using the concept of light rays subject to Snell's Law for a stratified medium. Alternatively we may apply Huygens's wave theory

according to which, in passing over the iceberg, the higher parts of the wave front move faster than the lower parts causing it to bend downwards.

Mutatis Mutandis similar phenomenon can apply to sound waves whose speed increases with increasing absolute temperature above zero, T , as $T^{\frac{1}{2}}$. During a warm sunny day therefore, when the temperature is typically hotter near the ground due to the sun's rays, the sound waves should be bent upwards. On a clear night, when the temperature near the ground drops rapidly by radiative cooling, sound waves should be bent downwards allowing distant sources, such as cars on a motorway, to be heard much more clearly than during the day. One of us, living as he does a kilometre or so away from the A14, which is, judged by the amount of traffic it carries effectively a motorway, had until recently always supposed that it was this temperature effect that was responsible for the din experienced at times when contemplating the night sky in his garden. However, the temperature effect should be isotropic,

Emails: g.w.gibbons@damtp.cam.ac.uk, c.m.warnick@damtp.cam.ac.uk

Pre-print no. DAMTP-2011-11

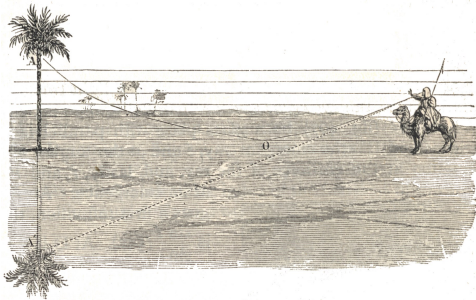


Figure 1: A 19th century woodcut showing a mirage in the desert. *Source: 'Éléments de Physique', Ganot*

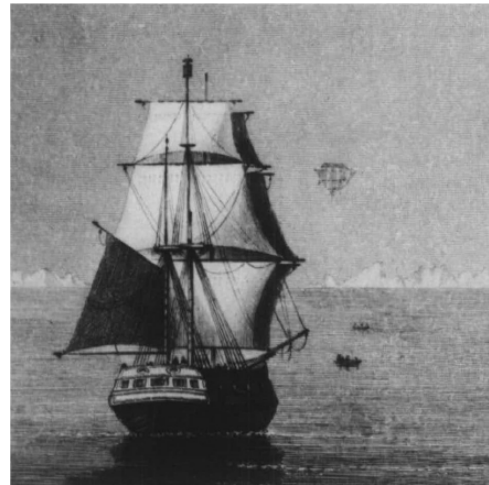


Figure 2: Etching of a sketch by the explorer William Scoresby, showing an arctic mirage. *Source: 'The life of William Scoresby', Scoresby-Jackson*

in other words it should affect the noise of cars coming from all directions and including those on less busy but closer city roads. The greater volume and speed of traffic on the A14 alone should not be so overwhelming.

The obvious directional influence is that of the wind. However, the speed of sound $v_s \approx 1250$ km per hour is so much greater than typical wind speeds $v \approx 30$ km per hour that simple convection of sound waves by the wind cannot be responsible for any significant directional effect. As pointed out to one of us by a colleague, Hugh Hunt, who made a similar point in the New Scientist of 15th April 2009 in response to readers' queries, it is not the wind velocity, but its gradient, that is its *variation with height*, called *wind shear* or more technically *vorticity* which is important. As is clear from observing clouds, wind speeds, while remaining roughly horizontal and much slower than the speed of sound, increase quite sharply with height, while remaining roughly horizontal. Thus it is not just the increased velocity $|\mathbf{v}|$ that matters, but its gradient or vorticity $\boldsymbol{\omega} = \text{curl } \mathbf{v}$.

Of course, examination of the literature shows that this is not a new observation and many papers and textbooks contain a simple

qualitative discussion. The earliest we have discovered dates from 1857 [1] and is due George Gabriel Stokes (1819-1903) who was appointed to the Lucasian Chair of Mathematics in Cambridge in 1849 and held it until his death 54 years later. His explanation, elaborated on by Osborne Reynolds (1842-1912) in 1874 [2], followed very closely Huygens's explanation for refraction by a gradient in the refractive index. If the wind direction is towards us, and the wind speed increases with height, the higher parts of the wave front move faster than the lower parts and the wave front is bent over towards us. If on the other hand the wind direction is in the opposite direction, the wave front will be bent upwards and hence away from us. The net effect is that if the vorticity $\boldsymbol{\omega}$ is non zero, the sound rays are deflected in an analogous way to the deflection of a charged particle of mass m and charge e by the Lorentz Force due to magnetic field \mathbf{B} . In fact this is not just an analogy but, as we shall see shortly, a precise correspondence for low wind speeds:

$$\boldsymbol{\omega} \equiv -\frac{e}{m}\mathbf{B}. \quad (1)$$

Note that since it is the velocity gradient that matters, it is not the direction of the wind at

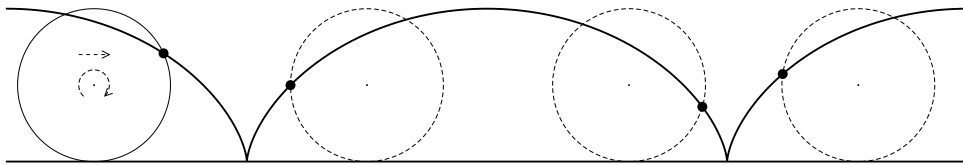


Figure 3: The cycloid, as traced out by a point on the circumference of a rolling circle

the ground or at a height above, but their difference which is important. In practice however, the speed of the wind is almost always much slower near the ground than above, and so usually it is the velocity at higher altitudes which matters. Thus, in principle there are two effects acting, and which is the more important depends on which induces the greater curvature κ to the sound rays. As Stokes and Reynolds realised $\kappa \approx \frac{1}{n} \frac{\partial n}{\partial z} = \frac{1}{2} \frac{1}{T} \frac{\partial T}{\partial z}$ for the thermal effect and $\kappa \approx \frac{1}{v_s} \frac{\partial v}{\partial z}$ for the wind shear, where n is the index of refraction. It is probably no coincidence that Stokes's work followed shortly after the first demonstration, by the German physicist Karl Friedrich Julius Sondhauss (1815 - 1886) in 1853 [3], that a balloon filled with CO_2 will act as a sound lens, focussing the sound of a ticking watch so as to render it audible some distance away.

Examples of the interplay of these two effects, which can cause sound to travel over large distances, abound. In early June, 1666, during the war between the Dutch and the English, both Samuel Pepys and John Evelyn reported in their diaries that while the sound of gun fire from ships off the coast of Kent could be heard clearly in London, it was not audible at all at the ports of Deal or Dover. As Pepys at the time observed:

“This ... makes room for a great dispute in Philosophy: how we should hear it and not they, the same wind that brought it to us being the same that should bring it to them.”

Infrasound (sound of very low frequency) from the volcanic explosion of Krakatoa on August 27 1883 was heard to travel several times around the earth. During the first world war,

the noise of the very large guns on the Western Front was often audible within a range of a 100 km or so, and often beyond 200 km, but not within a “zone of silence” between 100 and 200 km. On September 21, 1921 there occurred an enormous explosion at Oppau on the Rhine and the same phenomenon was observed, see Figure 4.

One explanation for some of these phenomena is reflection of sound from a layer of air in the upper atmosphere with a higher sound velocity. The dependence of the velocity of sound in the atmosphere follows its temperature profile. In the absence of wind, the temperature (and hence velocity of sound) decreases under normal circumstances up to a height of about 10 km, remains constant up to roughly 25 km, then increases to around 50 km, where it has a local maximum, and then has a local minimum at about 80 km, see figure 5. A simple application of the law of refraction

$$n(z) \sin \theta(z) = \text{constant}, \quad (2)$$

where the local speed of sound $v_s(z) \propto \frac{1}{n(z)}$, reveals that sound rays can bounce off the maxima of $v_s(z)$ but can also be trapped at the minima. Presumably the latter effect was responsible for the long distance propagation of infrasound from Krakatoa. A similar phenomena occurs for sound waves in the ocean. The speed of sound initially decreases with depth and then increases exhibiting a minimum value at a depth of around 1 km at the so-called SO-FAR channel. This allows whales to communicate over very large distances [8, 9] and more sinisterly, submarines to snoop on other submarines.

For simple profiles $n(z)$, the law of refraction (2) allows simple solutions for the rays. Thus if $n(z) \propto z$, one has catenaries with the

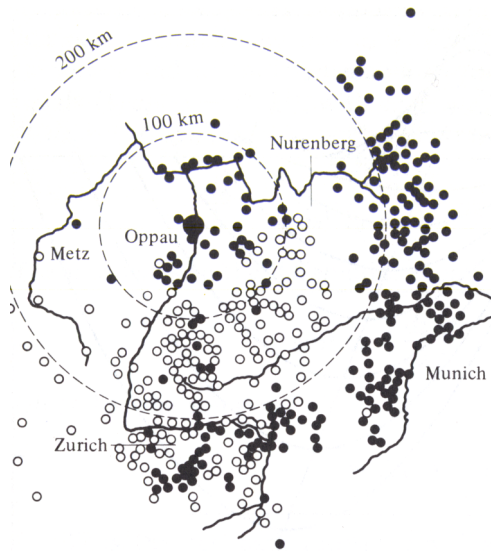


Figure 4: The explosion at Oppau, 1921. Filled circles represent locations where the explosion was heard and empty circles locations where nothing was heard

Source: 'Strange sounds in the Atmosphere: Part I', R. K. Cook, *Sound* 1, 12-16 (1962).

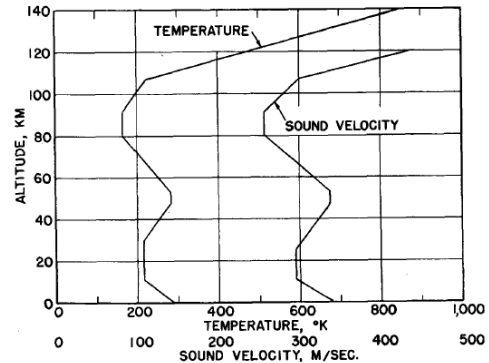


Figure 5: The variation of temperature and sound speed with altitude

horizontal axis $z = 0$ as the directrix. This gives a rough description of mirages in the desert. If $n(z) \propto \frac{1}{\sqrt{z}}$, the rays are cycloids, the curve traced out by the point on the circumference of a circle rolling without slipping along the horizontal axis (see Figure 3). One can imagine this as the path of a glow-worm sitting on the rim of a bicycle wheel as it rolls along in the dark. This could describe the rays passing over icebergs in the arctic. More importantly for what follows later, this can also be achieved by assuming that $n(z) \propto \frac{1}{z}$, in which case the rays are semi-circles centred on the horizontal axis. The addition of the effects of wind complicates considerably this simple picture.

Considering for a moment fundamental physics, one of the clearest trends in research over the last 100 years or so has been what one might call the *geometrisation* of physics. This is by no means a new phenomenon. Plato's association of the regular, or Platonic, solids with the classical elements is perhaps the earliest at-

tempt to explain the world through geometrical intuition. Geometry, in the modern sense of differentiable manifolds, really caught hold in physics in 1915 with Einstein's general theory of relativity. Since then, the use of geometry has accelerated. Modern string theory, with its 10 space-time dimensions and complicated internal 6-dimensional Calabi-Yau manifolds is perhaps the clearest example of this geometrisation process.

A geometrical approach has much to recommend itself, even to describe the more concrete physics we have thus far been considering. In this article, we will discuss how the properties of sound and light rays can be considered in a geometrical light. We will be interested in the behaviour of solutions of the wave equation¹ in a moving medium:

$$\left[\left(\frac{\partial}{\partial t} - W^i \frac{\partial}{\partial x^i} \right)^2 - c^2 h^{ij} \frac{\partial^2}{\partial x^i \partial x^j} \right] u(x, t) = 0. \quad (3)$$

¹Throughout this paper we will use the convention that indices $i, j = 1 \dots n$ which are repeated should be summed over

Here h^{ij} is related to the speed of sound in a direction parallel to the unit vector m_i by $v_{\mathbf{m}} = c(h^{ij}m_im_j)^{-1/2}$ and W^i is a vector giving the velocity of the medium at each point. We will be interested in particular in disturbances with short wavelength, which move along *rays*. We will start by considering the case of a static medium, $W^i = 0$. The geometry of the rays in this case is well known and we shall describe some of its properties and give some examples. We will then move on to the case of a moving medium and demonstrate that this can also be described geometrically, as we showed in [5]. We will have to loosen slightly our notion of a geometry in order to do so but the type of geometry which arises, a Finsler geometry, is very natural. In fact, this geometry first arose in our studies of light rays near rotating black holes. The link between the effects of gravity on light rays and refraction of light and sound waves by media can be made explicit and is the basis for much current work on optical and acoustic black holes. These analogue models for black holes allow experimentation in a laboratory, which would of course not be possible with real black holes. For this reason, a thorough understanding not just of the mechanisms of refraction, but the *geometry* of refraction is of great relevance both for terrestrial and celestial physics.

2 Geodesics and Fermat's Principle

2.1 Optical and Acoustic Geometries

The elementary theory of mirrors and lenses is largely concerned with tracing the paths of *light rays* on reflection (*Catoptrics*) or refraction (*Dioptrics*) at a surface. Although the Greeks were uncertain whether light proceeds from the eye to the object (*emission theory*) or from the object to the eye (*intromission theory*), and whether its passage is instantaneous or at a finite speed, nevertheless Heron of Alexandria (c.10-70 AD) was able to formulate the laws of reflection in terms of a *Principle of Short-*

est Length from object to eye via the reflecting surface. The occurrence of *caustics* shows that there can be more than one path, not all of which are necessarily the shortest and more accurately we refer to the principle *Principle of Stationary Length*, that is the length of each ray is merely stationary among all neighbouring paths.

Despite important pioneering work by Ibn al-Haytham or Alhazen (965-c.1040) demolishing the emission theory and investigating refraction, it took longer to unravel the fundamental law of Dioptrics. It was not until independent work by Abu Sa'd al-'Ala' ibn Sahl (c.940-c.1000), Thomas Harriot (c.1560-1621) and Willebrord Snel Van Royen (1580-1626) that the familiar *Law of Sines* was established and Pierre Fermat (c 1601- 1665) formulated his unified *Fermat's Principle of Stationary Time*. The idea is that the slowness of the ray inside a medium is proportional to its refractive index n . Note that the finite speed of light was only demonstrated by Ole Roemer (1644-1710) using the eclipse of Jupiter's moon Io in 1676. The relation of the refractive index to the speed of light remained controversial until experiments by Armand Hippolyte Louis Fizeau (1819-1896), Fresnel Augustin-Jean Fresnel (1788-1827) and George Biddell Airy (1801-1892) in the nineteenth century finally established its velocity as $\frac{c}{n}$, where c is its speed in vacuo. According to the discredited *corpuscular theory* the opposite relation holds. Both theories give the same rays but the speed with which light follows the rays differs. It would be more accurate therefore to speak of *Fermat's Principle of Stationary Optical Path Length*, where the optical length of a path γ is given by

$$L = \int_{\gamma} n(\mathbf{x})|d\mathbf{x}|, \quad (4)$$

where we have allowed for the possibility that the refractive index may depend upon position, as for example it does in a vertical stratified medium such as we encounter discussing mirages. Fermat's principle becomes the *Variational Principle*

$$\delta L = \delta \int_{\gamma} n(\mathbf{x})|d\mathbf{x}| = 0. \quad (5)$$

By the time Fermat introduced this principle, Christiaan Huygens (1629-1695) had initiated his wave theory of light and derived Fermat's Principle from it. His derivation makes it clear that it is the optical length or optical distance which enters into all interference effects, and its therefore appropriate to say that all optical measurements measure *Optical Geometry*. By the same token, measurements using sound waves may be said to measure *Acoustic Geometry* and measurements using seismic waves, as on the earth or more recently the moon [10] to measure *Seismic Geometry*.

It is clear that these geometries will, in an inhomogeneous medium for which the dependence of n on \mathbf{x} is non-trivial, differ considerably from *Euclidean Geometry*. The existence of such *non-Euclidean Geometries* was first realised by pure mathematicians in the early part of the nineteenth century working on the foundations of geometry. For centuries, people had been attempting to derive, starting from the other axioms, Euclid's fifth axiom: that through any point not on a given line there is exactly one line parallel to the first. This seemed to them so obvious that it was "necessarily" true. Eventually they gave up, Johann Carl Friedrich Gauss (1777-1855) privately and János Bolyai (1802-1860) and Nikolai Ivanovich Lobachevsky (1792-1856) publicly, showed the existence of two other types of homogeneous and isotropic *Congruence Geometries*, Spherical and Hyperbolic. The first is easy to grasp in two dimensions since it is just the geometry of the standard sphere, S^2 with the stationary paths (or *geodesics*) being the great circles. Navigators, either by sea or air, have been using spherical geometry since at least the time of Columbus. It is not too difficult to imagine a sphere in one dimension higher and indeed if the refractive index were to vary as

$$n = \frac{n_0}{(1 + \frac{\mathbf{x}^2}{4R^2})} \quad (6)$$

the optical metric would be precisely that of three dimensional spherical space S^3 of radius $n_0 R$. The resulting optical device is known as Maxwell's Fish Eye Lens since all rays emanating from any point \mathbf{x}_e are circles which recon-

verge onto the antipodal point $\bar{\mathbf{x}}_e = \frac{\mathbf{x}_e}{|\mathbf{x}_e|^2}$. We can verify that the optical distance along a radial geodesic is given by:

$$\int_0^\infty \frac{n_0}{1 + \frac{r^2}{4R^2}} dr = \pi n_0 R, \quad (7)$$

which is finite. Because, for large enough $|\mathbf{x}|$, the refractive index n drops below unity, the construction of such a device would require the manufacture of a suitable "meta-material". A more practical device was invented by Rudolph Karl Luneburg (1903-1949) and has

$$\begin{aligned} n &= (2|\mathbf{x}|^2 - 1), & |\mathbf{x}| \leq 1; \\ n &= 1, & |\mathbf{x}| \geq 1. \end{aligned} \quad (8)$$

This will focus all rays incident on it a fixed direction to the point on the circumference in the opposite direction.

The radius of curvature of the Spherical Geometry given by (6) is $n_0 R$. To obtain Hyperbolic Space H^3 , often called *Bolyai-Lobachevsky space* or just *Lobachevsky Space*, one needs only to let the radius of curvature become pure imaginary which leads to

$$n = \frac{n_0}{(1 - \frac{\mathbf{x}^2}{4R^2})}. \quad (9)$$

The refractive index becomes infinite when $|\mathbf{x}| = 2R$ which should be thought of as the boundary at 'infinity' of hyperbolic space. In fact the reader may easily verify that the optical distance along a radial path from the origin $\mathbf{x} = 0$ to the boundary at infinity is, by contrast with the case of spherical space, infinite.

Jules Henri Poincaré (1854-1912) gave a simple analogy which illuminates the roles played by the flat Euclidean metric geometry for which $n = 1$ and the curved non-Euclidean geometry for which n is given by (9) as follows. Imagine a medium whose temperature varies with radius as $\frac{1}{n}$ occupying a ball of radius $|\mathbf{x}| = 2R$, as measured by a measuring rod made from a substance such as Invar whose length is independent of temperature. If measured by a different ruler made of a material which expands in proportion to the temperature, then the rod will shrink to zero length as it approaches the the boundary which is at zero temperature. The boundary will thus seem to

be infinitely far away as measured by the second measuring rod. At the time that Poincaré wrote, people were still reeling under the discovery that what seemed to have been well established since antiquity: that Euclid's Geometrical Axioms were not logical necessities. There was thus great interest among geometers and philosophers as what was the “correct” or “real” geometry of space. For Poincaré it all depended upon how you measure it. He did however believe that one should always be able to find a system of measurements in which Euclid's Geometry holds.

Despite appearances both Spherical Geometry and Hyperbolic Geometry are, like their simpler Euclidean counterparts, both isotropic and homogeneous. For this reason they are candidates for the physical geometry of space, as measured for example by light rays in vacuo. Indeed according to Einstein's theory of General Relativity just these three possibilities can arise in the theory of the *Expanding Universe* proposed by Alexander Alexandrovich Friedman (1888 -1925) and Monsignor Georges Henri Joseph Édouard Lemaître (1894 - 1966). For many years cosmologists have been attempting to decide which best fits the observed universe. Based on observations of the Cosmic Microwave Background (CMB), and other data, the consensus now is that it is flat Euclidean geometry.

Of course no realistic medium is exactly homogeneous or isotropic, and in particular the speed of light, or sound, may depend upon direction as well as position. A familiar example is provided by bi-refringence in crystals such as calcite for which the ordinary and extra ordinary ray have different refractive indices, n_o and n_e . This more general situation may be taken into account using a more general geometry invented by Georg Friedrich Bernhard Riemann (1826 - 1866) called *Riemannian Geometry* in which the optical or acoustic path is given by

$$\delta L = \delta \int_{\gamma} \sqrt{h_{ij}(x_k) \frac{dx^i}{dt} \frac{dx^j}{dt}} dt = 0, \quad (10)$$

where h_{ij} is, in three spatial dimensions, a 3×3 symmetric array called the *metric tensor*. In-

deed one frequently introduces what is called a *line element* which is an expression for the infinitesimal form of a generalised Pythagoras's theorem: the infinitesimal distance ds between points x^i and $x^i + dx^i$ is given by

$$ds^2 = h_{ij}(x_k) dx^i dx^j. \quad (11)$$

Thus, for example, in the case of a uniaxial bi-refracting medium with unit field \mathbf{n} in the ordinary direction the *Joets-Ribotta* optical metric is [4]

$$ds^2 = n_e^2 d\mathbf{x}^2 + (n_0^2 - n_e^2)(\mathbf{n} \cdot d\mathbf{x})^2. \quad (12)$$

Riemann's ideas are fully incorporated into Einstein's Theory of General Relativity. Indeed, for a static spacetime a simple form of Fermat's Principle holds which, for example, allows one to discuss the optics of black holes in terms of an effective refractive index (in so-called isotropic coordinates)

$$n(\mathbf{x}) = \left(1 + \frac{GM}{2c^2|\mathbf{x}|}\right)^6 \left(1 - \frac{GM}{2c^2|\mathbf{x}|}\right)^{-2}, \quad (13)$$

where M is the mass and G is Newton's constant. In these coordinates, the black hole event horizon is located at $|\mathbf{x}| = \frac{1}{2} \frac{GM}{c^2}$. Note that, because the refractive index becomes infinite there, the event horizon is at infinite optical distance. A closer examination reveals that as one approaches the event horizon, the optical geometry approximates more and more closely that of hyperbolic space near its boundary at infinity as described above. We have recently pointed out that this is a universal feature of all static (“non-extreme”) event horizons and used it as a quantitative tool for discussing some of their puzzling physics [7].

Riemann also invented an even more general form of geometry, taken up by Paul Finsler (1894-1970) called *Finsler Geometry* in which a more general expression replaces (11) and this also arises in the optics and acoustics of moving media as we shall discuss presently. In the meantime we wish to say more about hyperbolic geometry, and in particular the hyperbolic plane H^2 .

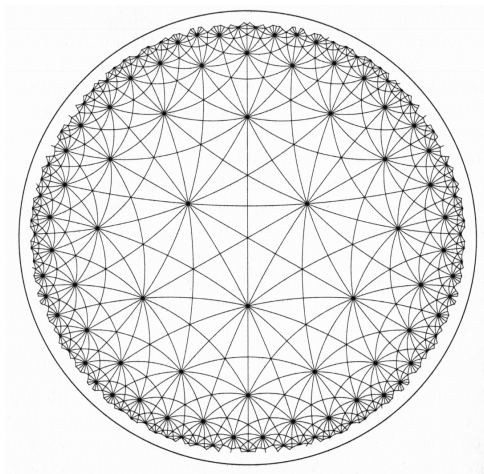


Figure 6: A tiling of the Poincaré disk. The edges of the triangles are geodesics.

Source: *Three Dimensional Geometry and Topology*, Thurston

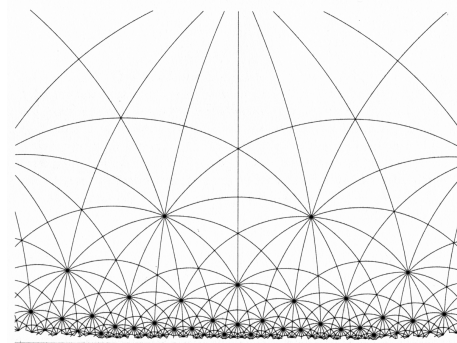


Figure 7: The same tiling, this time shown on the upper half-plane model of hyperbolic space.

2.2 The Hyperbolic Plane

The geometry of the hyperbolic plane is intimately connected with that of the complex numbers. Their introduction dramatically simplifies many formulae. To see this we adopt units in which the radius of curvature $n_0 R$ is set to unity. We further set $\mathbf{x} = 2R(x_1, x_2, x_3)$, $n_0 = 1$ in (9). The *Hyperbolic Plane*, H^2 , is obtained by setting $x_3 = 0$. In order to exploit the complex numbers we define $z = x_1 + ix_2$ to get

$$ds^2 = 4 \frac{dx_1^2 + dx_2^2}{(1 - x_1^2 - x_2^2)^2} = 4 \frac{|dz|^2}{(1 - |z|^2)^2}. \quad (14)$$

In this representation of the hyperbolic plane, the *Poincaré Disc*, H^2 occupies the interior of the unit disc $|z| = 1$ and one may verify that its geodesics are circular arcs which cut the unit circle at right angles. A tiling of H^2 by triangles whose edges are geodesics is shown as Figure 6. The triangles are all similar, so one can see how the apparent length of a measuring rod shrinks as we approach the boundary.

We are free, in addition, to perform a coordinate transformation to an equivalent form. We choose a complex coordinate $w = u + iv$ re-

lated to z by a *fractional linear transformation*

$$w = i \frac{1 + z}{1 - z}. \quad (15)$$

This maps the unit disc into the *Poincaré Upper Half Plane*, $v > 0$. The centre of the unit disc maps to the point $w = i$ and the boundary of the unit disc to the real axis $v = 0$. In these coordinates the line element becomes

$$ds^2 = \frac{|dw|^2}{\left| \frac{w - \bar{w}}{2} \right|^2} = \frac{du^2 + dv^2}{v^2}. \quad (16)$$

Because, as is easily verified, fractional linear transformations take circular arcs to circular arcs, the geodesics are again circular arcs. Because holomorphic maps are angle preserving, the geodesics are in fact semi-circles orthogonal to the real axis. Figure 7 shows the upper half plane tiled with the same geodesic triangles as in Figure 6.

Let's now think of u as horizontal distance and v as vertical height in an horizontally stratified medium in which the refractive index n decreases with height. If we assume that over a certain range of heights, v , to a good approximation

$$n \propto \frac{1}{v} \quad (17)$$

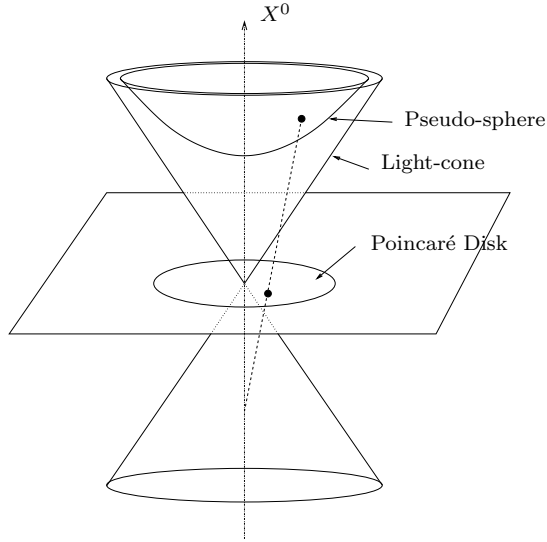


Figure 8: The hyperbolic plane as the pseudo-sphere in Minkowski space. Also shown are the light-cone $\mathbf{X} \cdot \mathbf{X} = 0$ and the plane $X^0 = 0$.

the rays will be semi circles. In this way we can easily explain the mirage mentioned in the introduction, that in arctic or antarctic regions light is bent over icebergs and ships behind icebergs are observed to float upside in the air above. To account for the mirages seen in the desert or on hot days driving on motorways in which trees or cars seem to be reflected in pools of still water, it suffices to take the complex conjugate and work in the lower half plane.

Of course many laws of horizontal stratification $n = n(v)$ will give qualitatively similar results, but there is a considerable economy to be made by adopting the law (17). If we do then the line element (16) is invariant under all fractional linear transformations taking the upper half plane into itself. These are of the form

$$w \rightarrow \frac{aw - b}{cw - d}, \quad ad - bc = 1, \quad (18)$$

where a, b, c, d are real. This defines the three dimensional group $SO(2, 1) \equiv SL(2, \mathbb{R})/\mathbb{Z}_2$ isomorphic with the Lorentz Group of three di-

mensional Minkowski spacetime. This is no accident. Much as it is convenient to think of the usual 2-sphere as the set of points at a fixed distance from the origin in Euclidean 3-space, there is a similar interpretation of hyperbolic space as a *pseudo-sphere* in Minkowski space. We consider the space \mathbb{R}^3 , but instead of the usual dot product, we endow it with the Minkowski product:

$$\mathbf{X} \cdot \mathbf{Y} = -X^0Y^0 + X^1Y^1 + X^2Y^2 \quad (19)$$

where $\mathbf{X} = (X^0, X^1, X^2)$ and similarly for \mathbf{Y} . For a vector with $\mathbf{X} \cdot \mathbf{X} > 0$, which we call *spacelike*, we can define the length to be $|\mathbf{X}| = \sqrt{\mathbf{X} \cdot \mathbf{X}}$. The hyperbolic plane of radius R is the set of points defined by

$$\mathbf{X} \cdot \mathbf{X} = -R^2, \quad X^0 > 0. \quad (20)$$

The pseudo-sphere is sometimes referred to as the *mass-shell*. This is because when we interpret the Minkowski spacetime as the geometry of special relativity in two spatial dimensions², the vectors with $\mathbf{P} \cdot \mathbf{P} < 0$ represent momentum vectors of particles whose rest mass, m , is given

²In this case we work in units where the speed of light is 1 and a particle of energy E and momentum (p_1, p_2) in the two spatial dimensions would have momentum vector $\mathbf{P} = (E, p_1, p_2)$.

by $\mathbf{P} \cdot \mathbf{P} = -m^2$. The mass-shell thus represents all the possible velocities for a particle of a given rest mass. It is possible to check that any vector tangent to this surface is spacelike, so that the Minkowski inner product allows us to define the length of such a vector. The geometry of this surface with this definition of length is that of the hyperbolic plane. A Lorentz transformation leaves both the Minkowski metric and the condition (20) unchanged and so represents an isometry of the hyperbolic plane. To recover the Poincaré disk model, we stereographically project the pseudosphere from the point $(-1, 0, 0)$ onto the plane $X^0 = 0$ as shown in Figure 8.

3 Zermelo's Problem and Finsler's geometry

3.1 Zermelo's navigation problem

In the previous section, we considered the problem of finding the ray paths of a sound wave propagating in a static medium. We showed how Fermat's principle of stationary time leads us to consider the geodesics of a Riemannian metric. We would now like to consider how sound waves propagate through a moving medium. Fermat's principle continues to apply, however we must work a little harder in order to translate the principle into a mathematical statement.

We will start off by considering a problem proposed by Ernst Zermelo in 1931. Suppose a boat, which can sail at a constant rate relative to the water on which it sits, wishes to navigate from point A to point B as quickly as possible. If the water is at rest, then the captain should steer along a straight line joining A to B . More generally, the captain should steer along a geodesic if the surface of the water may not be taken to be flat, for example if the points A and B are far enough apart that the Earth's curvature should be taken into account. The navigation problem for the captain in this case corresponds to finding the geodesics of some Riemannian metric.

Now let us suppose that the body of water on which the boat sits is not at rest, but instead moves with some velocity $\mathbf{W}(\mathbf{x})$, which we call the drift. The absolute velocity of the boat is now the sum of two components: the motion of the boat relative to the water, \mathbf{v} , and \mathbf{W} . In order to find the fastest route between A and B the captain must clearly take the drift into account. In order to do this, let us first consider the simplest situation, where the surface of the water is a plane and the drift \mathbf{W} is a constant vector, not changing from point to point. This situation is shown in Figure 9. We will assume for convenience that the speed of the boat relative to the water is c , a constant. We will also assume that the speed of the drift is less than the speed of the boat relative to the water, i.e. $\mathbf{W}^2 < c^2$. Let's define $\mathbf{d} = \vec{AB}$ and work out how long it will take the boat to get from A to B assuming that \mathbf{v} is constant. In this case, the position of the boat relative to A at time t will be

$$\mathbf{x} = t(\mathbf{v} + \mathbf{W}). \quad (21)$$

Supposing that the boat arrives at B at time T , we have

$$\mathbf{d} = T(\mathbf{v} + \mathbf{W}). \quad (22)$$

We wish to solve for T as a function of \mathbf{d} and \mathbf{W} . We can do this easily by looking at the equations we get from dotting both sides of (22) with \mathbf{W} and \mathbf{d} :

$$\begin{aligned} \mathbf{d} \cdot \mathbf{W} &= T(\mathbf{v} \cdot \mathbf{W} + \mathbf{W}^2), \\ \mathbf{d}^2 &= T^2(\mathbf{v}^2 + 2\mathbf{v} \cdot \mathbf{W} + \mathbf{W}^2). \end{aligned} \quad (23)$$

Noting that $\mathbf{v}^2 = c^2$ and eliminating $\mathbf{v} \cdot \mathbf{W}$ between the equations gives

$$T[\mathbf{d}] = \sqrt{\frac{\mathbf{d}^2}{c^2 - \mathbf{W}^2} + \frac{(\mathbf{d} \cdot \mathbf{W})^2}{(c^2 - \mathbf{W}^2)^2}} - \frac{\mathbf{d} \cdot \mathbf{W}}{c^2 - \mathbf{W}^2}. \quad (24)$$

The condition that the speed of the drift is less than c guarantees that the denominators are positive and that $T[\mathbf{d}] \geq 0$, with equality only when \mathbf{d} vanishes. We notice that if $\lambda > 0$, then $T[\lambda \mathbf{d}] = \lambda T[\mathbf{d}]$. We can also check that T obeys a *triangle inequality*:

$$T[\mathbf{d}_1 + \mathbf{d}_2] \leq T[\mathbf{d}_1] + T[\mathbf{d}_2]. \quad (25)$$

This means that the time T which we have found is in fact the *least* time to travel between

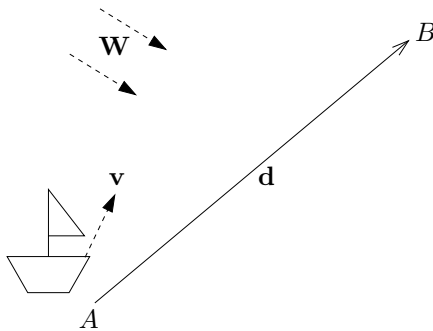


Figure 9: Zermelo's navigation problem with a uniform drift

A and B , because we cannot reduce the time by travelling along the sides of a triangle with base AB . A simple limiting argument shows that any curve from A to B will take longer to traverse than T .

Now we can consider a more general problem, where the boat is navigating in a Riemannian manifold M , with metric $h = h_{ij}dx^i dx^j$. The drift is a vector field $W^i(x)$ on M , which may vary from point to point and whose length is always less than c . Suppose the captain steers the boat so as to travel along a curve $\gamma(s)$, with $\gamma(a) = A$, $\gamma(b) = B$. In order to find the time taken to traverse this curve, we can approximate it with lots of straight sections on which the metric and the drift are roughly constant. We have worked out how long it takes to travel along such a line segment and we can simply add these times up. Passing to a limit, we find that the time taken to travel from A to B along this curve is

$$T[\gamma] = \frac{1}{c} \int_a^b F[\gamma^i(s), \dot{\gamma}^i(s)] ds \quad (26)$$

where

$$\begin{aligned} F[x^i, y^i]/c &= \sqrt{\alpha(x^i, y^i)} + \beta(x^i, y^i) \\ \alpha &= \frac{h_{ij}y^i y^j}{c^2 - W^2} + \frac{(h_{ij}y^i W^j)^2}{(c^2 - W^2)^2} \\ \beta &= -\frac{h_{ij}y^i W^j}{c^2 - W^2}, \end{aligned} \quad (27)$$

with $W^2 = h_{ij}W^i W^j$. This problem seems somewhat artificial as imagining a boat navigating a general curved space is rather strange.

This set up is very natural, however, in the context of sound rays. If h_{ij} is the acoustical metric of a material (so that a ray moving in the direction of the unit vector n^i moves with velocity $c/\sqrt{h_{ij}n^i n^j}$) and W^i is a bulk motion of the material, then T tells us the time the sound would take to travel along γ . We are now in a position to make a mathematical statement of Fermat's principle for a sound wave propagating through a moving medium. The sound rays are the paths which extremise the time along the path, or equivalently the optical length, $L = Tc$:

$$\delta L = c\delta T = 0. \quad (28)$$

Before we discuss what this means for the study of sound waves in a moving atmosphere, we will first discuss briefly a larger class of problems which have a similar form to ours.

3.2 Finsler and Randers geometry

We have thus far been speaking somewhat loosely about geometries, without describing exactly what we mean. For our purposes, the particular type of geometry which is of interest is a *Finsler geometry*. Although named after Paul Finsler, the concept of a Finsler geometry was introduced by Riemann in the same lecture that he proposed what is now known as Riemannian geometry. The defining feature of a Finsler geometry is that for suitably well behaved curves, one can define a curve length. In order to do so, one first has to define a *Finsler function*. The function F of (27) is a special

case. A Finsler function, in addition to an assumption on its smoothness, is required to have three properties

1. *Positivity*: $F[x, y] \geq 0$, with equality only if $y = 0$
2. *Homogeneity*: $F[x, \lambda y] = \lambda F[x, y]$, for $\lambda \geq 0$
3. *Subadditivity*: $F[x, y_1 + y_2] \leq F[x, y_1] + F[x, y_2]$

Given a Finsler function F , we can then define the length of a curve from $\gamma(a)$ to $\gamma(b)$ by:

$$L[\gamma] = \int_a^b F[\dot{\gamma}^i(s), \dot{\gamma}^i(s)] ds. \quad (29)$$

Condition 1 ensures that the length of any non-trivial curve is positive. Condition 2 ensures that the length of a curve does not depend on its parameterisation. Condition 3 is necessary so that the problem of finding curves of minimal length is well posed. This means that we can talk about the *geodesics* of F as being curves of minimal length between two points. Note that the ‘length’ defined in this way by the F of the previous section is *not* the usual length of the curve, so the geometry defined by this F differs from the Euclidean geometry of the plane.

Whilst Riemannian geometry is fairly well understood, Finsler geometry in general is much less well studied. This is mainly because of the sheer variety of possible Finsler functions, which can be very exotic. One of the simplest classes of Finsler function, into which our function F of the previous section falls, are the *Randers metrics*. The Finsler function of a Randers metric is given in terms of a Riemannian metric a_{ij} and a one-form b_i as

$$F[x, y] = \sqrt{a_{ij}(x)y^i y^j} + b_i(x)y^i. \quad (30)$$

This is a good Finsler function provided $a^{ij}b_i b_j < 1$, where a^{ij} is the matrix inverse of a_{ij} . One reason to study Randers metrics becomes apparent when we consider the equations satisfied by a curve which is a critical point of (29) when a_{ij} is the flat metric in \mathbb{R}^3 . Since we are free to choose the parameterisation, we can

assume that for the curve $\mathbf{x}(s)$ we have $\dot{\mathbf{x}}^2 = 1$ and we then find that $\mathbf{x}(s)$ is a critical point when

$$\ddot{\mathbf{x}} = \dot{\mathbf{x}} \times (\nabla \times \mathbf{b}). \quad (31)$$

We see that $\mathbf{x}(s)$ follows the path of a particle of mass m and charge e moving in a magnetic field $\mathbf{B} = m/e(\nabla \times \mathbf{b})$ with unit speed. For this reason, the extreme curves of L are sometimes referred to as *magnetic geodesics*. For a general a_{ij} , we find the generalisation of the Lorentz force law in a curved space, with b_i acting as the vector potential for the magnetic field. By extending the notion of a metric to allow Finsler geometries, we have brought the problem of charged particles in a magnetic field into the realm of pure geometry.

3.3 A uniform magnetic field in the Hyperbolic Plane

As an interesting example, we take $x^1 = u$, $x^2 = v$, with $v > 0$, and we will consider the Randers metric given by (30) with:

$$a_{ij} = \frac{\rho^2}{v^2} \delta_{ij}, \quad b_1 = \frac{\alpha}{v}, \quad b_2 = 0. \quad (32)$$

Where $\rho > 0$ and α are fixed real numbers. This is a good Finsler metric, provided that $|\alpha|/\rho < 1$. If $\alpha = 0$, we see that this Randers metric in fact corresponds to the Riemannian metric considered in §2.2, that of the hyperbolic plane of radius ρ in its ‘upper half-plane’ form. If α is non-zero, b corresponds to a vector potential for the magnetic field which is everywhere directed straight out of the plane and which has strength $B = \alpha/\rho$, independent of position. Thus the geodesics of this Randers metric will correspond to a charged particle moving in a uniform magnetic field in the hyperbolic plane. In order to find the geodesics, we have to find curves $(u(s), v(s))$ which extremise the length

$$L = \rho \int ds \left(\frac{\sqrt{\dot{u}^2 + \dot{v}^2}}{v} + \frac{\alpha}{\rho} \frac{\dot{u}}{v} \right). \quad (33)$$

Such a curve must satisfy the *Euler-Lagrange* equations:

$$0 = \frac{d}{ds} \left(\frac{\dot{v}}{v\sqrt{\dot{u}^2 + \dot{v}^2}} \right) + \frac{\sqrt{\dot{u}^2 + \dot{v}^2}}{v^2} + \frac{\alpha}{\rho} \frac{\dot{u}}{v^2},$$

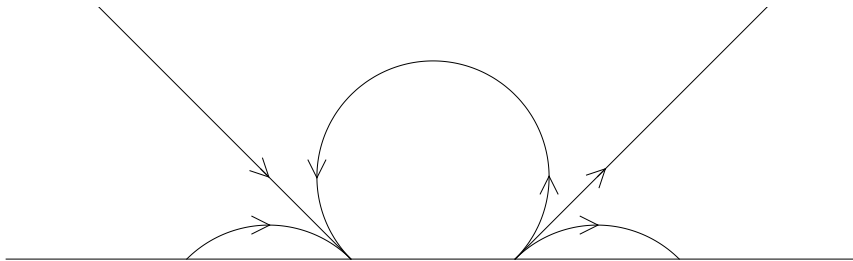


Figure 10: Some geodesics of the Randers metric given in (32), with $\alpha/\rho = 1/\sqrt{2}$.

$$0 = \frac{d}{ds} \left(\frac{\dot{u}}{v\sqrt{v^2 + \dot{u}^2}} + \frac{\alpha}{\rho} \frac{1}{v} \right). \quad (34)$$

In the case where $\alpha = 0$, we know from above that the geodesics are circles which meet the line $v = 0$ at right angles. We also know that when we have a constant magnetic field in the usual Euclidean plane that the particle trajectories are circles. It seems reasonable then to guess that with α non-zero, the geodesics remain circular. We can consider a possible solution of the form

$$\begin{aligned} u(s) &= u_0 + r \cos s \\ v(s) &= v_0 \mp r \sin s. \end{aligned} \quad (35)$$

Notice that the circle is traversed in a *clockwise* or *anti-clockwise direction* respectively for the two choices of sign. For a general Finsler metric, unlike for a Riemannian metric, the direction of travel is important and a curve will only be a geodesic when traversed in a particular direction. Substituting into (34) we find that we can satisfy the equations provided

$$\frac{v_0}{r} = \frac{\alpha}{\rho} = \pm B. \quad (36)$$

Thus for $0 < B < 1$ we can either have clockwise circles with centres above $v = 0$ or anti-clockwise circles with centres below $v = 0$. Since $B < 1$, we can interpret both cases geometrically as meaning that circles which meet the line $v = 0$ at an angle $\theta = \cos^{-1} B$ are geodesics, provided they are traversed in the appropriate sense. Taking a limit where r, v_0 get larger and larger with their ratio fixed, we find that straight lines making an angle θ with

the $v = 0$ axis are also geodesics, provided again that they are traversed in the correct direction. A little more work shows that in fact any geodesic of this Randers metric is one of these curves. Figure 10 shows examples of the various cases for $B = 1/\sqrt{2}$. For $B < 0$, we can simply reverse the sense of the curves.

4 Sound in a wind

We noticed in §3.1 that Fermat's principle tells us that a sound ray in a medium with acoustic metric h_{ij} with a wind W^i will move along a geodesic of a related Randers metric defined by

$$\begin{aligned} a_{ij} &= \frac{h_{ij}}{c^2 - W^2} + \frac{W_i W_j}{(c^2 - W^2)^2}, \\ b_i &= -\frac{W_i}{c^2 - W^2}, \end{aligned} \quad (37)$$

where $W^2 = h_{ij} W^i W^j$ and $W_i = h_{ij} W^j$.

Let's firstly consider what this means in the case where the speed of sound is constant and equal everywhere to c and the wind speed W is small in magnitude compared to c . This is a reasonable approximation for sound waves in a realistic atmosphere. Typically $W/c < 0.03$ and even in the strongest hurricanes, W/c does not exceed 0.3. For a constant, isotropic, speed of sound, the acoustic metric is simply

$$h_{ij} = \delta_{ij}. \quad (38)$$

If we work to first order in w/c , then we find that

$$a_{ij} = \frac{1}{c^2} \delta_{ij}, \quad \mathbf{b} = -\frac{\mathbf{W}}{c^2}. \quad (39)$$

Making use of (31) and keeping track of the factors of c , we find that the path followed by a sound ray is that of a particle of mass m and charge e moving with speed c in a magnetic field given by

$$\mathbf{B} = -\frac{m}{e}(\nabla \times \mathbf{W}) = -\frac{m}{e}\boldsymbol{\omega}, \quad (40)$$

where $\boldsymbol{\omega}$ is the vorticity of the wind. This justifies our assertion in equation (1) that the vorticity of the wind acts like a magnetic field on the sound rays.

A simple consequence of this correspondence is observed by seismologists measuring the oscillations of the Earth after a large earthquake. The spectral peaks are split by the Earth's rotation. From our magnetic point of view, the effect of the rotation is to give rise to a constant magnetic field inside the Earth. The splitting of the spectrum is in precise analogy with the Zeeman effect which gives rise to a splitting of spectral lines for atoms in a magnetic field.

4.1 A stratified example

An interesting problem to study involves combining a varying speed of sound with a wind in a stratified atmosphere. We can gain some insight by investigating a particular choice of acoustic metric and wind. Let's suppose that the acoustic metric for the medium at rest is the hyperbolic metric discussed previously

$$ds^2 = h_{ij}dx^i dx^j = l^2 \frac{dx^2 + dz^2}{z^2} \quad (41)$$

We'll take this to model sound rays in an atmosphere varying with temperature near the ground, which we assume to be at $z = l$. The speed of sound at ground level is given by c . We'll suppose there's a horizontal wind with strength proportional to height, so that

$$\mathbf{W} = (-w\frac{z}{l}, 0). \quad (42)$$

Where w is some fixed parameter with units of velocity. We can easily calculate the associated Randers metric and find the time to go along a

curve $(x(s), z(s))$. It is best expressed in terms of new variables:

$$u = \frac{cx}{l\sqrt{c^2 - w^2}}, \quad v = \frac{z}{l}. \quad (43)$$

This just represents a rescaling of the axes both parallel and perpendicular to the ground. In terms of u, v , the time is given by

$$T = \frac{l}{\sqrt{c^2 - w^2}} \int ds \left(\frac{\sqrt{\dot{u}^2 + \dot{v}^2}}{v} + \frac{w}{c} \frac{\dot{u}}{v} \right). \quad (44)$$

Thus, the sound rays follow the geodesics of a Randers metric of precisely the form we considered in §3.3, with B given by w/c !

As a simple application, we can consider the problem of tracing the sound emanating from a point source, P at ground level, which is at $v = 1$. We know that the sound rays in the u, v coordinates are circles (and lines) which meet the line $v = 0$ at an angle $\cos^{-1}(w/c)$. We also know that these circles have a clockwise sense if their centre is above $v = 0$ and an anti-clockwise sense if it's below. This is already enough information to draw the rays shown in Figure 11 for the particular value $w/c = 1/\sqrt{2}$. We sketch outward directed geodesics which have a common starting point, P . The straight line geodesic through P plays an important role as a *separatrix*, which separates two different behaviours for the trajectories. In this case, any ray emitted to the left of the separatrix will return to the ground to the left of P , while a ray emitted to the right returns to ground to the right. If we suppose that P is emitting sound uniformly in all directions, we see that more of the energy emitted is absorbed by the ground on the left of P than on the right. In this case three times as much, which we can see by considering the angle the straight geodesic makes with the ground.

This example has three free parameters: c , w and l . By choosing these appropriately, we can match (for example) the speed of sound, the speed of the wind and the wind shear at ground level to a real, more complicated profile. In fact, in [5] we showed that it is possible to construct a model based on the hyperbolic plane with four free parameters, so that one can

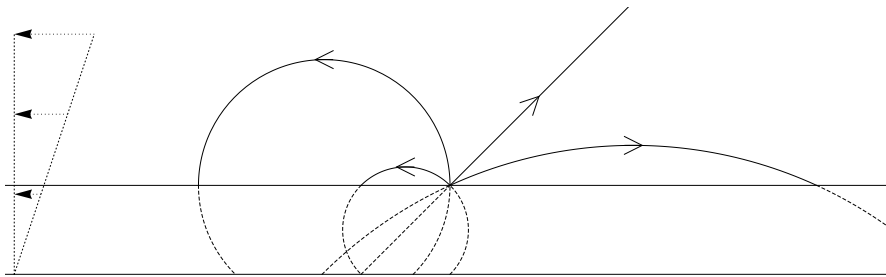


Figure 11: Some sound rays emanating from a point on the ground for $w/c = 1/\sqrt{2}, l = 1$. The wind velocity at various heights (including the hypothetical extension below ground level) is shown at the left of the diagram. The rays are shown extending as dashed lines below ground level to show that they meet $z = 0$ at an angle of $\pi/4$.

additionally set the rate of change of speed of sound with height at ground level as well.

5 Conclusion

In this article we have sought to show that the motion of a charged particle moving in two-dimensional Lobachevsky space, or the hyperbolic plane, equipped with a non-uniform magnetic field can provide a useful model for sound rays in a moving medium with a gradient in the refractive index. We have mentioned that in its three-dimensional version the geodesics of Lobachevsky space provide a useful model for the motion of light rays near the event horizon of a non-rotating black hole. If the black hole is rotating then Coriolis type effects, referred to in General Relativity as the rotation of inertial frames, provide an effective magnetic field. These two examples by no means exhaust the possible applications of hyperbolic geometry to physics.

Two-dimensional surfaces abound in nature and if they have negative Gauss curvature, sometimes called *anti-clastic* at a point, the surface cannot lie on one side of its tangent plane at that point. Thus a finite smoothly embedded surface without edges in Euclidean space cannot have everywhere negative Gauss curvature, but a finite portion of a surface with edges may. A simple example is provided by a holly leaf. An example of great current physical interest,

following the 2010 Nobel Prize to Andre Geim and Konstantin Novoselov is a graphene surface containing topological defects called *disclinations* in which some of the hexagonal lattice cells have been replaced by heptagons. The electrical and other properties of such surfaces are of great interest, and their study entails solving the Dirac equation in a portion of two-dimensional Lobachevsky space. The motion of charged particles on abstract finite Riemann surfaces with no boundary or edges which have constant negative curvature and uniform magnetic field are of interest in statistical mechanics since for weak magnetic field the motion is chaotic or *ergodic* as it is known technically. However as the magnetic field strength is increased there is a sudden phase transition and this ceases to be the case.

Three dimensional Lobachevsky space has been invoked to model some aspects of *quantum dots* and the physics of four and five dimensional Lobachevsky space and their conformal boundaries are currently of intense interest by String Theorists since Juan Maldacena suggested the famous *AdS/CFT correspondence* which has led to a number of break throughs in quantum gravity and the quantum theory of black holes. Without going into technical details, it may be of interest to outline some features of this fascinating idea. Both in Quantum Field Theory and in String Theory it is customary to work in *imaginary time*. Thus if we start

in Minkowski spacetime with spacetime metric

$$ds^2 = -c^2 dt^2 + d\mathbf{x}^2, \quad (45)$$

we can pass to Euclidean space with positive definite metric

$$ds^2 = c^2 d\tau^2 + d\mathbf{x}^2. \quad (46)$$

by setting

$$t = i\tau, \quad \tau \text{ real}. \quad (47)$$

Often calculations may be performed more easily in Euclidean space. We then pass back to Minkowski spacetime by setting

$$\tau = -it, \quad t \text{ real}. \quad (48)$$

This process is called a *Wick Rotation* and it also works for some curved spacetimes. A case in point is Anti-de-Sitter spacetime. This is a solution of Einstein's equations with a negative cosmological constant. It may be obtained from Lobachevsky space by a simple Wick Rotation. Maldacena's brilliant conjecture is that there is a precise correspondence between String Theory in Anti-de-Sitter spacetime on the one hand, and a special type of quantum field theory, called a Conformal Quantum Field Theory, on the other hand, the latter being defined on the conformal boundary of Anti-de-Sitter spacetime. The conformal boundary of Anti-de-Sitter spacetime is conformally related to Minkowski spacetime. If we "Wick rotate" this conjecture we are led to conjecture a correspondence between String Theory in Lobachevsky space and Quantum Field theory on its conformal boundary, the latter being conformally related to Euclidean space.

We hope that in this article we have made it clear that not only is a knowledge of hyperbolic geometry and Lobachevsky space useful for understanding traffic noise, but it has a much wider range of applications in theoretical physics; from cosmology to condensed matter physics to String Theory and Planck scale physics. We commend to the interested reader its study and further exploitation.

References

- [1] G. C. Stokes, On the Effect of Wind on the Intensity of Sound *Report of the British Association, Dublin* (1857) 22
- [2] O. Reynolds, On the Refraction of Sound by the Atmosphere *Proc Roy Soc A*, **22** (1874) 531-548
- [3] C. Sondhauss, On the Refraction of Sound, *Phil Mag* **30** 73-77
- [4] A. Joets and R. Ribotta, A geometrical model for the propagation of light rays in an anisotropic inhomogeneous medium *Optics Communications* **107** (1994) 200-204
- [5] G. W. Gibbons and C. M. Warnick, Traffic Noise and the Hyperbolic Plane, *Annals Phys.* **325** (2010) 909 [arXiv:0911.1926 [gr-qc]].
- [6] G. W. Gibbons, C. A. R. Herdeiro, C. M. Warnick and M. C. Werner, Stationary Metrics and Optical Zermelo-Randers-Finsler Geometry, *Phys. Rev. D* **79** (2009) 044022 [arXiv:0811.2877 [gr-qc]].
- [7] G. W. Gibbons and C. M. Warnick, Universal properties of the near-horizon optical geometry, *Phys. Rev. D* **79** (2009) 064031 [arXiv:0809.1571 [gr-qc]].
- [8] C. S. Morawetz, Geometrical Optics and the Singing of Whales *Amer Math Monthly* **85** (1978) 548-554
- [9] D. E. Weston and P.B. Rowlands, Guided acoustic waves in the ocean *Rep. Prog. Phys.* **42** (1979) 347-387
- [10] R. C. Weber et al. Seismic Detection of the Lunar Core *Science* (2011)

The Authors



Gary Gibbons was born exactly 300 years after Gottfried Wilhelm Leibniz. He came up to St. Catharine's College, Cambridge, to read Natural Sciences in 1965, specializing in Theoretical Physics. After taking Part III of the Mathematical Tripos he commenced research in DAMTP, first under D. W. Sciama and then S. W. Hawking. After various post-doctoral appointments he was appointed to a lectureship in DAMTP in 1980. He is now Professor of Theoretical Physics in DAMTP. He was elected to the Royal Society in 1999. He has been a Professorial Fellow of Trinity College since 2002.



Claude Warnick came up to Queens' College, Cambridge, in 2001 to read Mathematics. After completing Part III of the mathematical Tripos in 2005, he studied for a PhD in the General Relativity group of DAMTP, under Gary Gibbons. He has been a Research Fellow at Queens' since 2008.